 doi:10.20944/preprints202201.0355.v1

Article

Photocatalytic reduction of nitrates and combined photodegradation with ammonium

Francesco Conte[a], Veronica Pellegatta[a], Gianguido Ramis[b], Ilenia Rossetti[a,*]

[1] Chemical Plants and Industrial Chemistry Group, Dip. Chimica, Università degli Studi di Milano, CNR-ISTM and INSTM Unit Milano-Università, via C. Golgi 19, 20133 Milan, Italy
[2] Dip. Ing. Chimica, Civile ed Ambientale, Università degli Studi di Genova and INSTM Unit Genova, via all'Opera Pia 15A, 16145 Genoa, Italy
* Correspondence: ilenia.rossetti@unimi.it

Abstract: Bare titania and metal promoted TiO_2 catalysts were employed in the treatment of nitrates, which are ubiquitous pollutants of wastewater. The results show that the process can be carried out under visible light (from white light LED lamp) and, in the best case, 23.5% conversion of nitrate was obtained over 4 hours with full selectivity towards N_2 by employing 0.1 mol% Ag/TiO_2 prepared by flame spray pyrolysis. Moreover, the performance was worse when testing the same catalysts with tap water (11.3% conversion), due to the more complex composition of the matrix.

At last, it was found that the photoreduction of nitrate can be effectively performed in combination with the photo-oxidation of ammonium without loss in the activity, opening to the possibility to treat highly polluted wastewater with a single process. The latter treatment employs the two contaminants simultaneously as electron and holes scavengers, with very good selectivity, in a completely new process that we may call Photo-Selective Catalytic Reduction (Photo-SCR).

Keywords: Wastewater treatment; Nitrogen-containing pollutants; Nitrate photoreduction; SCR; Photocatalysis; Titania.

1. Introduction

Nitrogen mainly occurs in form of inert diatomic molecule, which can be converted into more reactive compounds through the biological nitrogen fixation cycle. However, it has been since the development of the Haber-Bosch process that we faced a massive production of substances that contain activated nitrogen such as ammonia and nitrates, which are commodities widely used in fertilisers formulation. These compounds have a huge impact on the cycle of nitrogen since the net conversion of N_2 from the atmosphere has been almost four-fold multiplied, with respect to the amount naturally fixed by the plants [1]. Moreover, traditional agriculture techniques does not employ efficiently the fertiliser, which is easily dispersed into the atmosphere, where inorganic nitrogen contribute to rain acidification and to NO_x formation [2], or leached from the soil by the rain and irrigation systems, then entering the water cycle from the groundwater where nitrogen containing compounds cause eutrophication and pollution due to their intrinsic toxicity to living organisms [3]. Furthermore, groundwater is one of the primary sources of drinking water, but the World Health Organisation (WHO) defines it "drinkable" only if it does not contain more than 50 ppm (parts per million) of NO_3^- and 3 ppm of NO_2^-, whereas the ammonia has not to exceed 500 ppb (parts per billion) [4]. Although these are critical thresholds, noxious effects have been observed even with lower concentration, especially for the smallest fishes and microorganisms [5], while for humans the daily usage of polluted water can lead to irritations, DNA damage, tumoral formation and disequilibria in body pH [6,7].

 doi:10.20944/preprints202201.0355.v1

Thus, when the pollutant concentration is higher than the value tolerated by the environment, it is necessary to treat the water source. For instance, contaminated water can be cleaned via biological denitrification, which is a safe process, effective in most cases. However, it requires to constantly feed the microorganisms with a suitable carbon source that is exploited by the latter to perform the reduction of nitrate to molecular nitrogen [8]. Furthermore, alternatives processes are the ion exchange chromatography, which can treat highly polluted streams but essentially create a more concentrated solution to dispose, or finer approaches such as ultrafiltration, reverse osmosis and electro-dialysis, for which the cost of the disposal is increased significantly [9,10].

We explore here an innovative photocatalytic approach which exploits appropriate semiconductors to absorb light and promote RedOx reactions through the photogenerated holes and electrons. In details, titanium dioxide is a largely employed material (safe, inexpensive and stable) and a well-known photocatalyst that absorbs in the ultraviolet region due its wide band gap, which depends on its polymorphs structure (3.0 eV for the rutile phase and 3.2 eV for anatase) [11–13]. Moreover, in form of nanoparticles, it has been used to promote several reactions such as degradation of organic pollutants, CO_2 activation, wastewater treatment and water splitting to produce hydrogen [14–16]. Anyway, as a photocatalyst, it is limited by its wide band gap and by the fast recombination between the photogenerated electrons and holes. To improve both aspects the properties of the catalyst can be tuned by deposition of metal co-catalysts over its surface, for instance Cu, Ag, Au, Pt: it is an established method to extend the lifetime of the photogenerated charges and to narrow the band gap, for instance thanks to the reduction treatment of the photocatalyst or for plasmonic surface resonance, thus allowing to operate under visible light [17]. This latter effect may be exploited through different effects. Some metals contribute to light absorption thanks to their own plasmonic resonance (*e.g.* Au). In other cases, the incorporation of the metal in the structure of the semiconductor can lead to doping. Finally, most of the exemplified metals are well known reduction catalysts, promoting the effective reduction of TiO_2 which is a well-known method to decrease titania band gap [18–20].

Furthermore, the band energies of titania, whose potential is -0.05 V for the conduction band and 2.7 V for the valence one, makes it a strong oxidising agent and a mild reducing one [21] and, in addition, they are suitable to perform either the photo-reduction of nitrite and nitrate or ammonium photo-oxidation, as the standard potential of the N_2/NH_3 couple is *ca*. 0.06 V whereas for the couples NO_3^-/N_2 and NO_2^-/N_2 it is respectively 1.25 V and 1.52 V.

In this study, we have evaluated the photocatalytic activity of several titania-based catalysts that were obtained either from commercial titania or homemade TiO_2 (prepared by flame spray pyrolysis) and promoted variously via metal co-catalysts addition. These materials were employed in the treatment of water solutions containing sodium nitrate at selected pH values, in the attempt to simulate wastewater composition, and the process was carried out under UV or visible light irradiation after optimization of the reaction parameters, with the aim of obtain an efficient and sustainable way to degrade the pollutant which can compete with the well-established water treatment techniques. The simultaneous abatement of ammonia and nitrates was also explored as a fully new process here called Photo-Selective Catalytic Reduction (Photo-SCR).

2. Results and Discussion

2.1. Materials characterization

Nitrogen adsorption and desorption isotherms were used to estimate the specific surface area and the pore volume of the catalysts (Figure 1). As reported in Table 1, the deposition of a co-catalyst generally caused an increase of the surface area and of pore volume of these materials, although the gain depends on the metal deposited and the temperature at which the reduction was performed after impregnation, the minimum

 doi:10.20944/preprints202201.0355.v1

effect being observed with Au. This is ascribed to the formation of agglomerates of particles inducing interparticle porosity (meso- and macro-), scarcely present in the bare material, constituted by dense nanoparticles poorly agglomerated. In addition, the catalysts supported on FSP titania showed higher surface area due to the smaller size of the particles compared to P25 ones. Moreover, the micropore pore volume of the metal-promoted catalysts was generally lower than the commercial benchmark (P25) and it is likely to be caused by pores blockage by the metal and a collapsing of the micropores that occurs during the reduction at high temperature.

Figure 2 illustrates the XRD patterns of selected materials. The latter shows two titania phases, anatase and rutile, with the anatase that accounts for the 70-87% of the whole structure. The content of anatase was generally lower for the FSP samples due to a possibly higher temperature of the flame during the synthesis or to a longer residence time in the hottest part of the flame. Anyway, the graph shows a small variation for those peaks associated with the main phases, thus the presence of a co-catalyst does not influence its phase composition. In addition, there are no clues of new peaks, and then other phases, due to the metal deposition. This is in line with the very low metal loading and its high dispersion.

DR-UV-Vis analysis was performed in order to calculate the band gap (BG) of the active materials. From Table 1, it is evident that the addition of a co-catalyst was effective in reducing the BG of the bare titania, which is about 3.41 eV and in the case of FSP titania with 0.1% of Au its value dropped to 3.11 eV, thus improving the absorption of visible light. This band gap reduction is here attributed to the reduction of the metallic co-catalysts at high temperature, which causes a partial reduction of the titania better catalysed by the presence of the metal itself.

Table 1. Results of the characterization analysis of selected catalysts.

0.1% Au/FSP	A(70)+R(30)	65	28	0.30	0.0003	16	3.11
0.1% Ag/FSP	A(70)+R(30)	72	30	0.36	0.00044	17	3.24
0.1% Pt/FSP	/	59	26	0.25	0.0037	19	/
FSP	A(65)+R(35)	68	24	0.14	0.02	20	3.23
1% Ag/P25	/	57	/	0.54	0.0052	36	3.15

Sample	P25	0.1% Pt/P25	0.1% Ag/P25	0.1% Au/P25
Phase %	A(78)+ R(22)	A(87)+R (13)	A(87)+R (13)	A(87)+R (13)
BET surface Area (m^2/g)	45	55	61	47
Crystallite size (nm)	15	21	21	21
Total pore volume (cm^3/g)	0.11	0.32	0.21	0.38
t-plot micropore volume (cm^3/g)	0.012	0.0036	0.0040	0.0026
BJH adsorption pore width (nm)	22	23	24	25
Band gap (eV)	3.41	3.12	3.23	3.27

doi:10.20944/preprints202201.0355.v1

 doi:10.20944/preprints202201.0355.v1

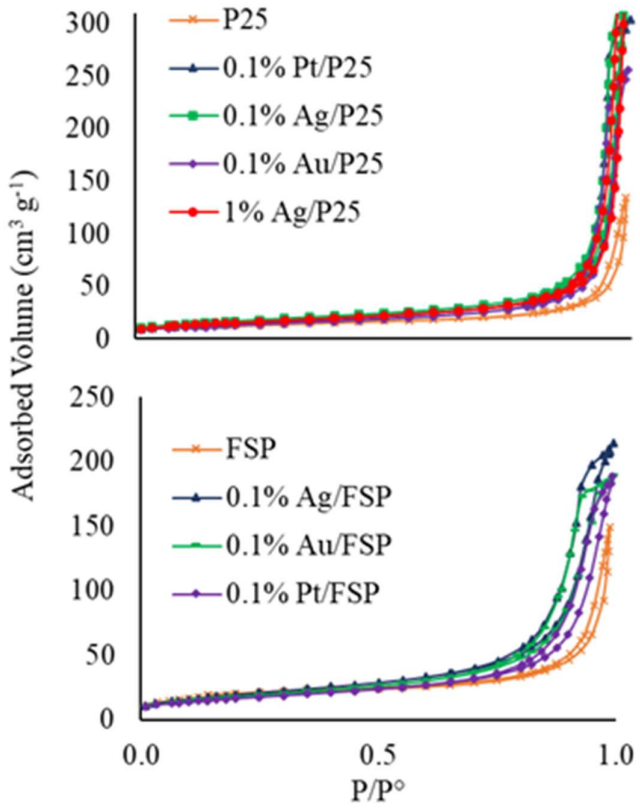

Figure 1. BET adsorption-desorption isotherms of selected catalysts. Adapted from [22]

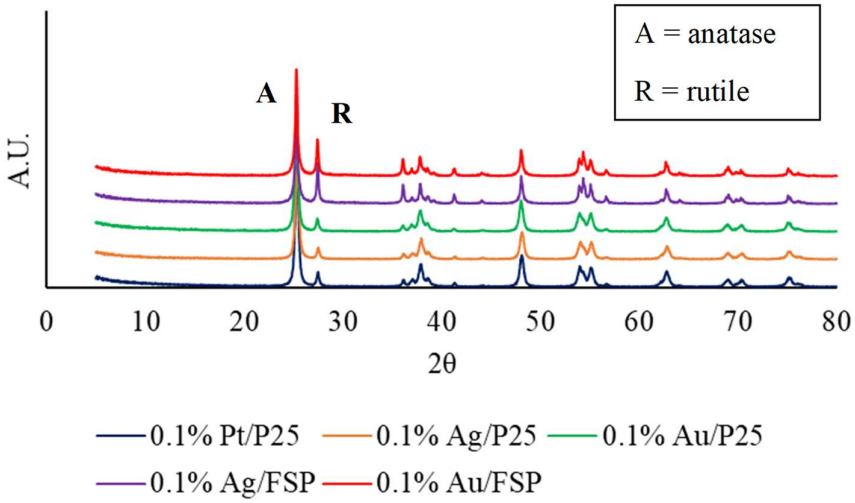

Figure 2. XRD characterization results for selected catalysts.

 doi:10.20944/preprints202201.0355.v1

2.2. Photo-reduction of nitrate promoted under UV light irradiation

The very first tests were carried out with the reactor in sealed configuration, using 0.1%Pt/FSP as active material, due to its good performance achieved in previous experiments [15], using an UV lamp as photons source. From the results of previous works [23], we decided to operate the treatment at pH 5, since slightly acidic values increased both the conversion of nitrate and the selectivity towards N_2. The solution was kept under irradiation for 24h in order to follow the time evolution of the reaction.

As reported in Figure 3, the conversion of the nitrate was moderate and did not exceed 25% after 24h of irradiation. Some ammonium was detected among the products, as the results of an overreduction [24]. Furthermore, looking at the trend of nitrogen evolution it seems that the catalyst is not so active in the early stage of the treatment, at least towards our target product, since appreciable amounts of N_2 were detected only after 5 hours of exposure. Overall, we measured a negligible selectivity towards NO_2^-.

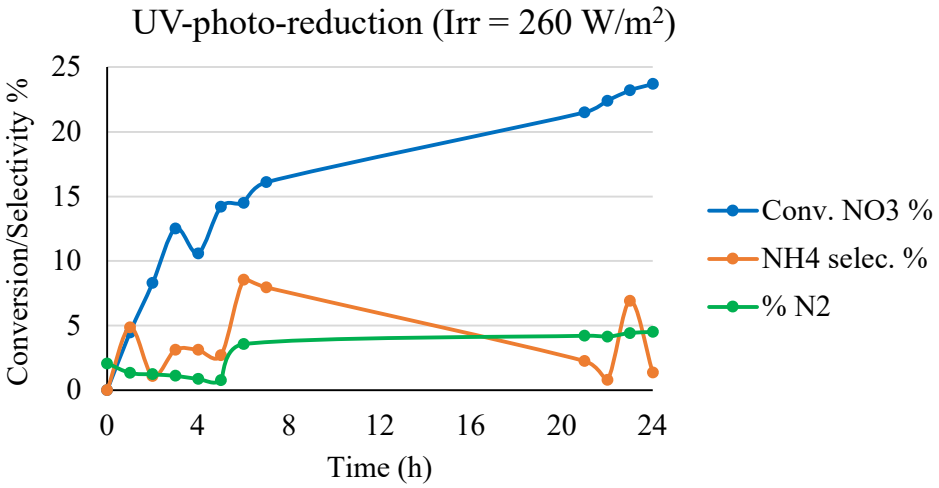

Figure 3. Photo-reduction of NO_3^- under UV irradiation (Irradiance = 260 W/m^2) with 0.1%Pt/FSP as photocatalyst (1 g/L), $NaNO_3$ (6 mM), pH 5, r.t. and 250 ml of solution (Reactor 1).

2.3. Photo-reduction under Visible light (LED)

The first parameter to be tuned was the concentration of pollutant. It was preferred to work with reactor 2, since measuring very low amounts of contaminant could increase significantly the experimental error. In addition, the 0.1%Ag/FSP catalyst was employed, already used in case of UV treatment [15], due to its low band gap which allows light absorption in the visible range.

As illustrated in Figure 4, the best results were obtained with a nitrate concentration of 1.7 mM, with a 23.5% conversion at the end of the treatment, which is an impressive result considering the low power of the LED lamp (about 30W) and that the incident photons have much less energy than the ones emitted by the UV lamp. Nevertheless, the deposition of reduced noble metals over the titania surface is well known to increase the harvesting of visible light by the photocatalyst [25].

Although higher concentration of reactant should favour the kinetics, in that case we are working with a photochemical treatment whose yield depends on the total number of

 doi:10.20944/preprints202201.0355.v1

irradiated photons, which is fixed, therefore working with lower concentration of substrate molecules causes higher conversion, while keeping the same amount of catalyst (activated equally by the incident photons). By contrast, if the NO_3^- concentration is too low, the reaction kinetics slows down unacceptably, thus, 1.7 mM was selected as the best $NaNO_3$ concentration for the following step, which was the optimization of the substrate/catalyst ratio. In order to find the best ratio, three tests were performed with values between 17-72 $mmol_{NO3-}/g_{cat}$ (Figure 5). Either increasing or reducing the amount of catalyst caused a drop below 14% of nitrate conversion. Lower amount of catalyst (72 $mmol_{NO3-}/g_{cat}$) was insufficient and actually an induction time before the beginning of the reaction was observed. On the other hand, higher amounts of titania (17 $mmol_{NO3-}/g_{cat}$) provide more active sites for adsorption and reaction, though it may hinder the passage of the light and determine a loss of activity. Also, in this case the intermediate value showed the highest conversion.

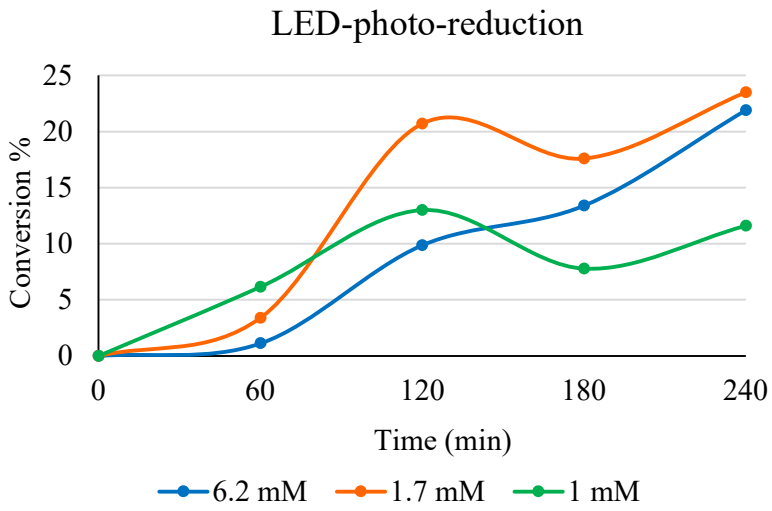

Figure 4. Photo-reduction of NO_3^- under LED lamp with 0.1%Ag/FSP as photocatalyst (0.034 mol_{NO3-}/g_{cat}), various concentration of $NaNO_3$ (1 – 6.2 mM), pH 5, rt and 1000 ml of solution (Reactor 2).

 doi:10.20944/preprints202201.0355.v1

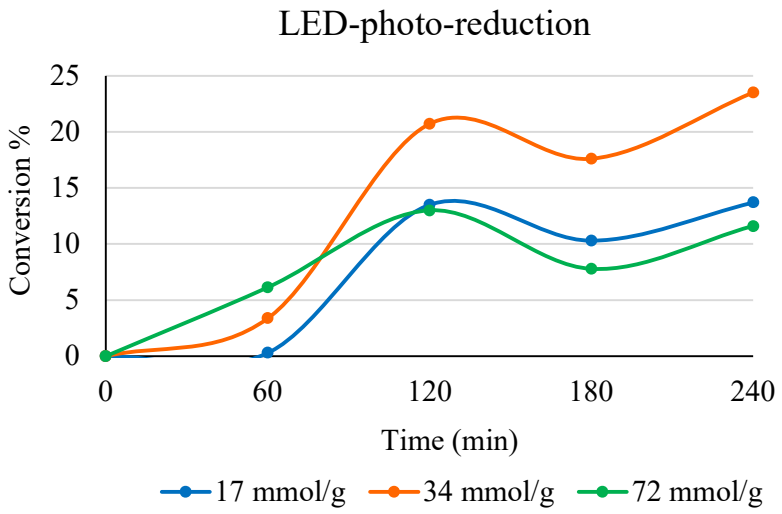

Figure 5. Photo-reduction of NO_3^- under LED lamp using 0.1%Ag/FSP as photocatalyst, with various substrate/cat ratio (17-72 $mmol_{NO3-}/g_{cat}$), $NaNO_3$ (1.7 mM), pH 5, rt and 1000 ml of solution (Reactor 2).

2.4. Comparison of different photocatalysts

Once the best conditions in which perform the reaction were found, a series of metal deposited catalysts were tested under LED white light irradiation. The results in terms of nitrate conversion are reported in Figure 6.a. Despite the expectations, the only catalyst which performed better than the bare P25 is the one loaded with silver resulting in a 23.5% conversion, whereas others material gave results between the 19% (0.1 Au/FPS) and 3% (0.1 Au/P25). In addition, a not negligible selectivity towards ammonium has been observed when treating the wastewater with P25 and 1% Ag/P25 (from Figure 6.b, *ca.* 13.5% in both cases), as well as 0.1% Au/FSP, although the latter showed a very little selectivity towards ammonium and nitrite just in the early stage of the process. Anyway, a possible explanation for the poor performance achieved with the functionalised catalysts is that the reduction of nitrate is in competition with other reactions such us the reduction of water to hydrogen. Indeed, this path is kinetically favoured due to the lower number of electrons involved, *i.e.* 2 *vs.* 10 for the couple NO_3^-/N_2, and, as reported by Challagualla *et al.* [26], the noble metals active in the hydrogen evolution are Pt, Pd due to the favourable position of their sub-bands which are located below the conduction band (CB), while Ag is more prone to nitrate reduction and release less hydrogen since sub-bands are far from CB. Unfortunately, the current photoreactor configuration operates in semi batch mode with He flow and/or open top, preventing the possibility to accumulate significantly and quantify the possibly evolved H_2.

 doi:10.20944/preprints202201.0355.v1

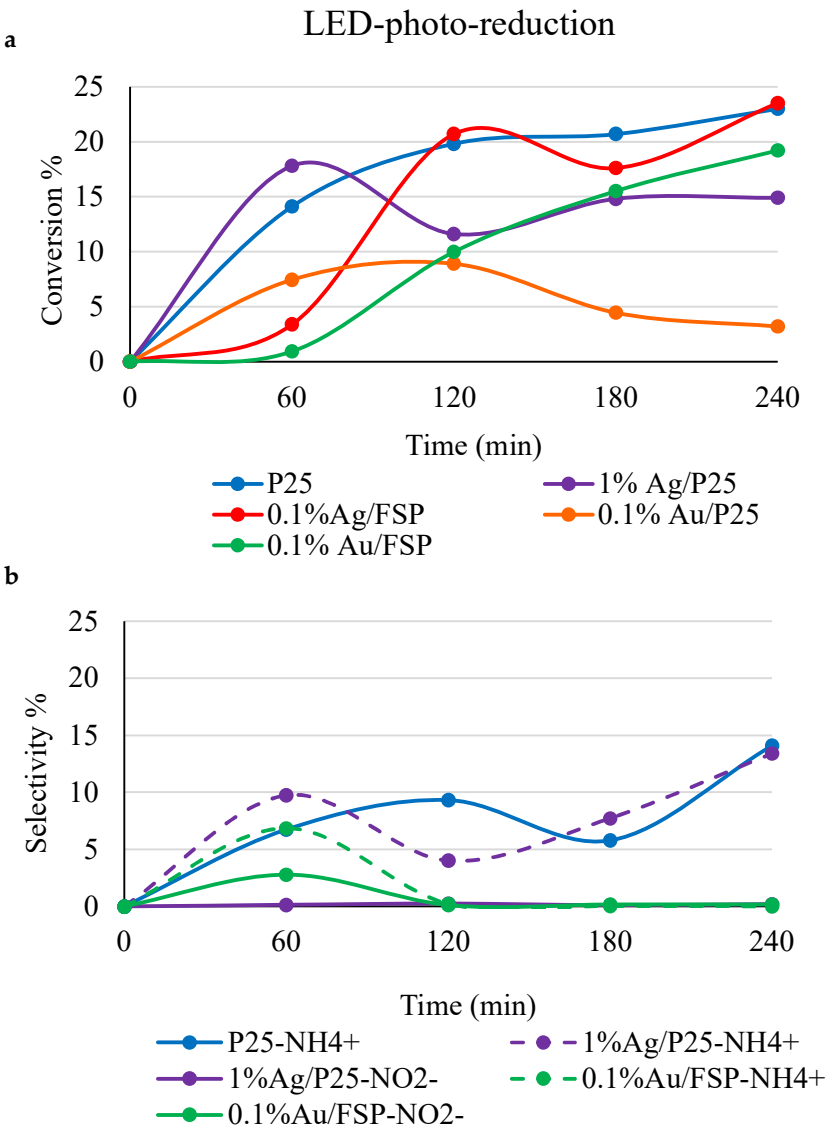

Figure 6. a) Conversion of NO_3^- under LED lamp with several photocatalyst, substrate/cat ratio 34 $mmol_{NO3-}/g_{cat}$, $NaNO_3$ (1.7 mM), pH 5, rt and 1000 ml of solution; **b)** Selectivity of the photocatalyst towards NH_4^+ and NO_2^-. The amount is negligible if not reported.

The photo-reduction of nitrate was performed also under UV light but using both the best conditions and the more active catalyst found in case of visible light studies. The following test was conducted with the UV reactor opened to air. Figure 7 shows a slightly better performance over the short period, with a 23.4% conversion of nitrate after 2 hours *vs.* the 8.3% of the platinum deposited catalyst. Moreover, there were no traces of over-reduced compounds as well as intermediates such as nitrite. However, a maximum in conversion was observed which subsequently reached a stable 20% plateau. These results agree to what reported in literature [27]. In addition, silver was preferred for the deposition since it was less expensive than platinum. Moreover, the test was repeated switching to a visible light source and the reaction time was increased to 24h, which revealed that the catalysts based on silver showed a trend similar to what was already observed with

Preprints (www.preprints.org) | NOT PEER-REVIEWED | Posted: 24 January 2022 doi:10.20944/preprints202201.0355.v1

0.1% Pt/FSP. Indeed, there is a maximum conversion of ammonium followed by a plateau for several hours, then the conversion rose again to reach its final value.

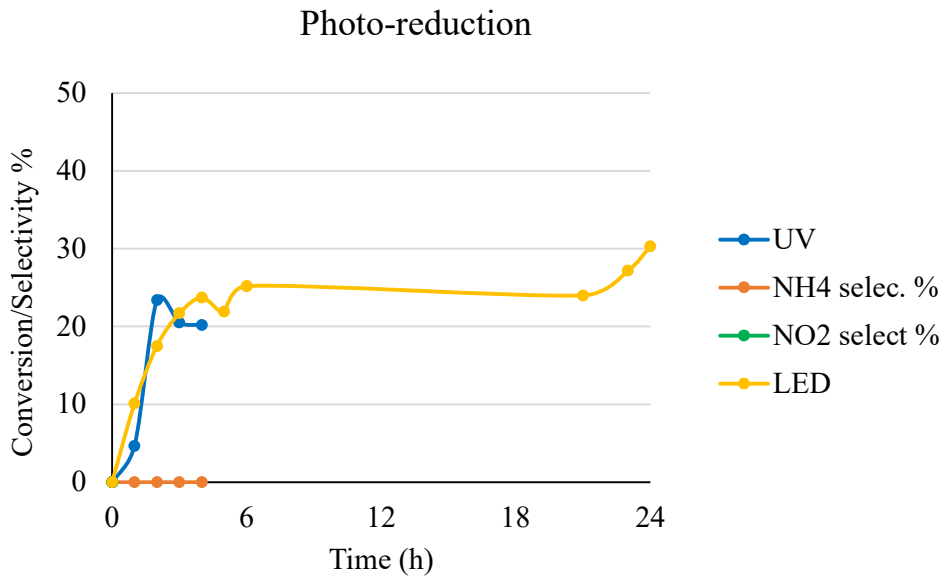

Figure 7. Photo-reduction of NO_3^- under UV lamp (Irr. 260 W/m²) or LED with 0.1%Ag/FSP as photocatalyst (substrate/cat ratio 34 $mmol_{NO3-}/g_{cat}$), $NaNO_3$ (1 mM), pH 5, rt, 250 ml (UV, Reactor 1) or 1000 mL (LED, Reactor 2) of solution

To conclude, we attempted to simulate a real wastewater by preparation of the nitrate solution with tap water. Figure 8 illustrates that the treatment of a real matrix causes a halving of the catalytic conversion of nitrates, since only 11.3% of the initial amounts of the substrate is mineralized to nitrogen, probably due to parasitic consumption of electrons by concurring species more prone to be reduced than the nitrate.

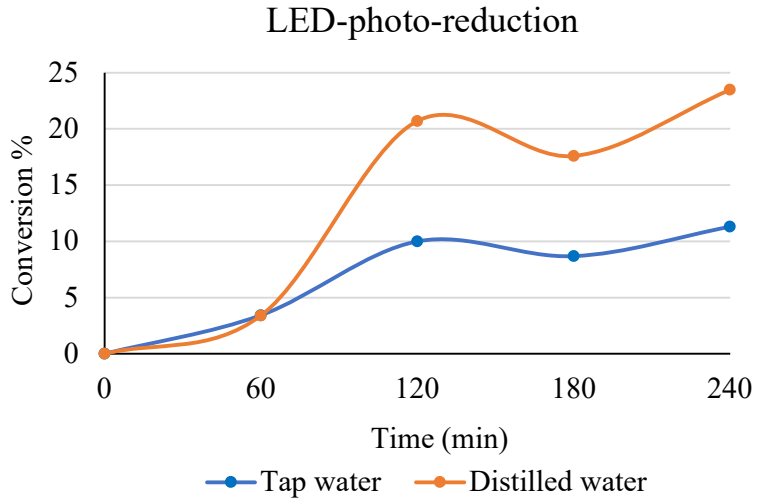

Figure 8. Photo-reduction of NO_3^- under LED lamp using 0.1%Ag/FSP as photocatalyst, substrate/catalyst ratio 34 $mmol_{NO3-}/g_{cat}$, $NaNO_3$ (1.7 mM), pH 5, rt and 1000 ml of solution prepared with distilled or tap water (Reactor 2)

 doi:10.20944/preprints202201.0355.v1

2.5. Combined photo-degradation under Visible light

When a photon of the proper wavelength is absorbed by the photocatalyst it promotes the formation of a photo-excited electron (e^-) and a hole (h^+). The first one is the reducing species which is involved in the photo-reduction of our substrate. However, the hole must be consumed in order to complete the redox reaction. Sometimes, a sacrificial agent (hole scavenger), such as oxalic or formic acid, is added to the reaction mixture since it is easily oxidised by the holes [27,28], preventing a charge accumulation and the fast recombination of the e^--h^+ couple that lowers the efficiency of the photocatalyst. On the contrary, our previous investigation on the use of HCOOH as HS led to the opposite conclusion, with decreasing nitrate conversion at increasing formic acid concentration [29]. Also, in this case we speculate that the presence of a more effective hole scavenger may favour parallel reactions, such as hydrogen production, which is unfortunately undetectable in the semi-batch configuration of our reactor. Besides this, it is not envisaged to add further reactants to treat wastewater, thus an alternative solution is here proposed.

We have recently demonstrated that the oxidation of ammonium can occur on the same titania-based catalyst employed so far and in the same conditions [22,23], then, a combined photo-treatment was performed to abate simultaneously both nitrate and ammonium. The ratio between the reactants was set to the stoichiometric and the degradation was performed in three configurations in order to boost the reactions. The results are reported in Figure 9 and firstly, they show that the conversion of both ammonium and nitrate is almost coincident in every stage of the treatment, therefore it is probable that both the Redox reactions benefit from each other. The first attempt was made using the LED lamp and it was found a reaction trend quite similar to the expectation, with a maximum of conversion around 2 hours of irradiation and a final conversion for both NH_4^+ and NO_3^- of about 20% after 4 hours. The nitrate conversion would be rate limiting in this case, since the literature data for photooxidation of ammonia report higher conversion. Overall, it is a promising result since the performance was not worse and two processes were carried out simultaneously. Slightly higher conversion, close to 30%, was achieved under UV irradiation, likely taking advantage of the presence of ammonium as hole scavenger.

Preprints (www.preprints.org) | NOT PEER-REVIEWED | Posted: 24 January 2022 doi:10.20944/preprints202201.0355.v1

Lastly, a third test was carried out with a constant air supply flowing through the solution. This setup returned a small increase in the reactor performance in case of photo-oxidation of ammonium [22]. However, Figure 9 clearly highlights a limited effect of this solution, as the conversion is only pushed up to a 22%.

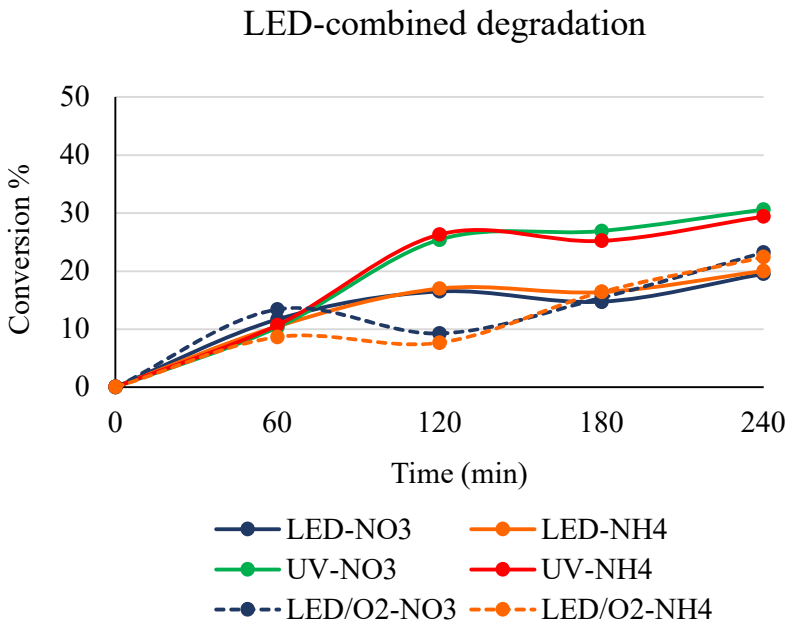

Figure 9. Photo-reduction of NO_3^- under LED or UV lamp using 0.05 g of 0.1%Ag/FSP photocatalyst, $NaNO_3$ (1.7 mM), NH_4Cl (2.8 mM), pH 5, rt and 1000 ml of solution (Reactor 2). LED test was repeated with air bubbling (air flow 12 mL/min).

3. Materials and Methods

3.1 Materials preparation

P25 is a commercial titania in form of nano powder supplied by Evonik [30]. It is generally constituted of uniform nanoparticles ca. 20 nm in diameter, with a mixed phase of anatase and rutile approximately 70:30. The specific surface area is typically 45-50 m^2/g and the powder is constituted of ca. 20 nm dense nanoparticles.

As a comparison, another flame-based technique, from a different precursor and leading to different calcination time and temperature was used. TiO_2 nanoparticles were prepared via flame spray pyrolysis (FSP) using a homemade apparatus yet described in details [30–32]. Briefly, the apparatus includes a burner with a hole in the centre that is ringed by many flamelets. The latter are fed with a mixture of methane and oxygen (0.5 L/min CH_4 and 1 L/min O_2), whereas in the central hole another current of oxygen (5 L/min) is supplied along with the precursor solution, which is usually prepared dissolving into xylene + propionic acid (1:1 v/v) the selected amounts of titanium isopropoxide (Sigma Aldrich, 97%). The solution is pumped at constant rate, for instance 2.7 mL/min, through a needle inserted from the bottom of the burner, then it is dispersed by the oxygen co-current into small drops that are instantly vaporised and burned by the flame. The catalyst in form of nano powder is then deposited over a glass bell which surrounds the burner. The FSP catalysts used in this work were obtained by application of a pressure drop at the nozzle of 1.5 bar.

Metal promotion of the catalysts was achieved through wet impregnation [16], which involves the formation of a clear solution in water by addition of the selected amount of

 doi:10.20944/preprints202201.0355.v1

metal precursor and titania to a round-bottom flask, then the solution is stirred for 2h and evaporated under reduced pressure until a homogeneous powder is obtained. Subsequently, the powder is dried in a static oven (105 °C) for one night and reduced in a tubular over under hydrogen flow (5°C/min of ramp and 3h at the maximum reduction temperature indicated in Table 2). The detailed amounts and conditions are reported in Table 2 and were selected after proper TPR analysis.

Table 2: Details for reparation of each catalyst through wet impregnation

Precursor	Metal to support ratio (%mol)	Support	Reduction T (°C)	Appearance
AgNO3 (Sigma Aldrich, >99%)	0.1	TiO2-FSP	150	Grey - Brown
AuCl3 (Sigma Aldrich, >99%)	0.1	TiO2-FSP	700	Light Purple
Pt(acac)2 (Sigma Aldrich, >97%)	0.1	TiO2-P25	700	Grey
AuCl3 (Sigma Aldrich, >99%)	0.1	TiO2-P25	700	Light purple
AgNO3 (Sigma Aldrich, >99%)	0.1	TiO2-P25	150	Grey - Brown
AgNO3 (Sigma Aldrich, >99%)	1.0	TiO2-P25	150	Dark - Grey

2.2. Materials characterization

Adsorption and desorption isotherms were obtained adsorbing N_2 over the active material at -196°C after overnight degassing at 150°C by means of a Micrometrics ASAP2020 apparatus.

X-ray diffraction patterns (XRD) were registered on a Rigaku D III-MAX horizontal-scan powder diffractometer equipped with Cu-K Kα radiation and a graphite monochromator on the diffracted beam.

Diffuse Reflectance (DR) UV-Vis spectra of samples were recorded on a Cary 500 UV-Vis NIR spectrophotometer (Varian instruments, Santa Clara, CA, USA) in the range of 200-800 nm.

2.3. Procedures and reactor setup

Two different photoreactors were used in this work. The first one (Reactor 1, Figure 10.a) is a cylinder-type round bottom reactor whose capacity is about 350 mL and which allows the insertion of a co-axial UV lamp from the top. It can be used in a sealed configuration, for instance to measure the nitrogen evolution, or open to air, as when an external white light LED lamp is employed. The second setup include a larger reactor (Reactor 2, Figure 10.b) with a volume of 3000 mL and it is mor suitable for external irradiation such as UV and LED. The latter is a spotlight-type lamp with a power of 30 W (Yonkers Insipre, 2700 lm) that has been fixed over the solution (100 mm). By contrast, the UV lamp employed was a medium pressure-type with one emitting bulb (Jelosil HG 100 AS, 125 W, maximum emission at 365 nm) and the irradiance measured with a photoradiometer (delta OHM HD2102.2) was *ca.* 260 W/m^2. External UV lamp irradiance is 116 W/m^2.

All the experiments were carried out selecting the proper reactor and adding the selected amount of photocatalyst, sodium nitrate and water. Then, the pH was adjusted with the minimum amount of diluted hydrochloric acid (0.002 M, from 37% solution). The treatment begun when the lamp was switched on.

The nitrogen evolution was monitored qualitatively by connecting the reactor to a gas chromatograph (HP 5890, Porapak Q + MS columns) and sampling with a 75 mL/min flow of helium.

The liquid phase was sampled with a glass syringe, then filtered (cellulose acetate filter, Sartorius Stedim, 200 nm) in order to remove the solid catalyst and analysed by means of an ion exchange chromatograph (Metrohm 883 Basic IC) equipped with an

 doi:10.20944/preprints202201.0355.v1

anionic column (Metrosep C 4 - 250/4,0) in series to a chemical suppressor, which reduces the background noise. The eluent is a water solution of Na_2CO_3 (3.2 mmol/L, 99.5%) and $NaHCO_3$ (1 mmol/L, 99.7%). Moreover, the ammonium possibly formed by over-reduction was analysed with the same instrument after switching to a cationic column (Metrosep A Supp 4 - 250/4,0) with the proper eluent, which contains HNO_3 (1.7 mmol/L, from 70% solution) and dipicolinic acid (0.7 mmol/L, 99.0%) diluted with HPLC water.

All the chemical reagents were purchased from Sigma Aldrich as supplied, without further purification.

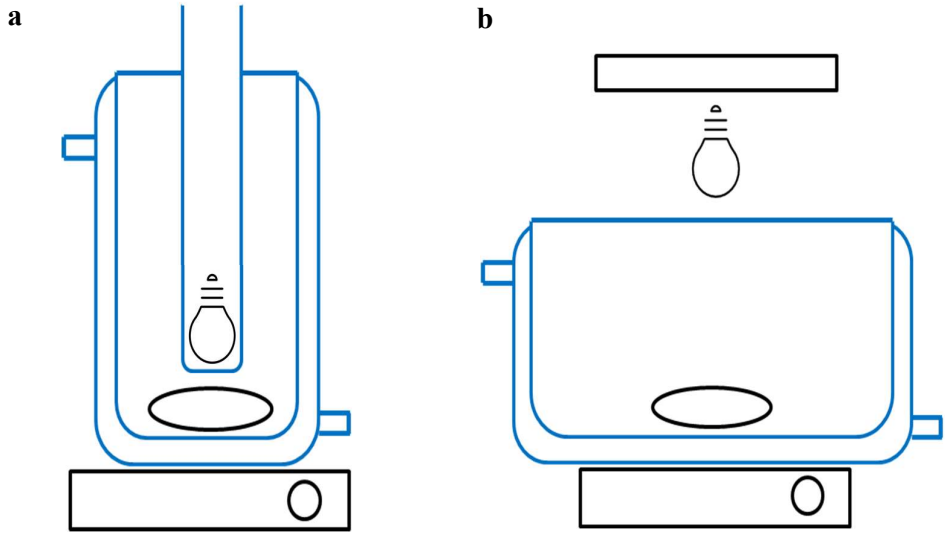

Figure 10. Reactor scheme a) immersed lap (UV) and b) external lamps (UV and LEDs)

4. Conclusions

The photo-abatement of nitrate has been successfully carried out under both UV and visible light irradiation using titania based photocatalysts. Firstly, both the irradiation sources employed allowed gave conversion between 30 and 20%, depending on the catalyst. No advantages support the usage of the UV lamp instead of the LED one, since the latter consumes less power (30 W vs 125 W), releases less heat and lasts longer. Moreover, under visible light it was found that the most active catalyst was the FSP titania loaded with 0.1%mol of Ag, although it only performed a bit better than bare titania. Other metals of an increase of co-catalyst loading depressed the catalyst performance.

The conversion with 0.1% Ag/FSP dropped from 23.5% to 11.3% when using tap water, likely because of multiple species that compete to react with the photogenerated electrons. On the other hand, the photo-reduction can be effectively performed in combination with photo-oxidation of ammonium, which is a fully new field of investigation that allows the concomitant abatement of two pollutants.

Author Contributions: Conceptualization, I.R. and G.R.; methodology, F.C.; investigation, V.P.; resources, I.R and G.R.; data curation, F.C.; writing—original draft preparation, F.C.; writing—review and editing, I.R. and G.R.; supervision, I.R.; project administration, I.R.; funding acquisition, I.R. All authors have read and agreed to the published version of the manuscript.

Funding: This research was funded by Fondazione Cariplo (Italy), grant number 2015-0186 "DeN – Innovative technologies for the abatement of N-containing pollutants in water".

I. Rossetti is grateful to Fondazione Cariplo and Regione Lombardia for financial support through the grant 2016-0858 – "Up-Unconventional Photoreactors".

Data Availability Statement: All the relevant data are reported in this article.

Conflicts of Interest: The authors declare that they have no conflict of interest.

References

[1] Rockström J, W. Steffen, K. Noone, Å. Persson, F. S. Chapin, E. F. Lambin, et al. A safe operation space for humanity. Nature 2009;461:472–5.

[2] Driscoll CT, Whithall D, Aber JD, Boyer E, Castro M, Cronon C, et al. Nitrogen Pollution: Source and Consequences in the U.S. Northeast. Environment 2003;45:22.

[3] Chislock M, Doster E. Eutrophication: Causes, Consequences, and Controls in Aquatic Ecosystems. Nat Educ … 2013:1–8.

[4] Herschy RW. Water quality for drinking: WHO guidelines. World Health Organization; 2012. https://doi.org/10.1007/978-1-4020-4410-6_184.

[5] Camargo JA, Alonso A, Salamanca A. Nitrate toxicity to aquatic animals: A review with new data for freshwater invertebrates. Chemosphere 2005;58:1255–67. https://doi.org/10.1016/j.chemosphere.2004.10.044.

[6] Volkmer BG, Ernst B, Simon J, Kuefer R, Bartsch G, Bach D, et al. Influence of nitrate levels in drinking water on urological malignancies: A community-based cohort study. BJU Int 2005;95:972–6. https://doi.org/10.1111/j.1464-410X.2005.05450.x.

[7] Pyatt FB. Potential effects on human health of an ammonia rich atmospheric environment in an archaeologically important cave in southeast Asia. Occup Environ Med 2003;60:986–8. https://doi.org/10.1136/oem.60.12.986.

[8] Park JY, Yoo YJ. Biological nitrate removal in industrial wastewater treatment: Which electron donor we can choose. Appl Microbiol Biotechnol 2009;82:415–29. https://doi.org/10.1007/s00253-008-1799-1.

[9] Nur T, Shim WG, Loganathan P, Vigneswaran S, Kandasamy J. Nitrate removal using Purolite A520E ion exchange resin: batch and fixed-bed column adsorption modelling. Int J Environ Sci Technol 2015;12:1311–20. https://doi.org/10.1007/s13762-014-0510-6.

[10] Ferro S, Australia E. Removal of nitrates from highly-contaminated industrial wastewater Sustainable Environmental Technology for Chemical and Allied industries (SETCA) View project Innovative Technologies for the Remediation of Soils and Waters View project. La Chim e l'Industria 2012:100–10.

[11] Rek-Lipczynska A. Purification of the Air in the Historic Cities of Towns. IOP Conf. Ser. Mater. Sci. Eng., vol. 471, 2019. https://doi.org/10.1088/1757-899X/471/10/102029.

[12] Fujishima A, Rao TN, Tryk DA. Titanium dioxide photocatalysis. J Photochem Photobiol C Photochem Rev 2000. https://doi.org/10.1016/S1389-5567(00)00002-2.

[13] Royal Society of Chemistry. TiO2 : Manufacture of Titanium Dioxide. RSC Adv Chem Sci 2016.

[14] Banerjee S, Dionysiou DD, Pillai SC. Self-cleaning applications of TiO2 by photo-induced hydrophilicity and photocatalysis. Appl Catal B Environ 2015;176–177:396–428. https://doi.org/10.1016/j.apcatb.2015.03.058.

[15] Bahadori E, Tripodi A, Ramis G, Rossetti I. Semi-Batch Photocatalytic Reduction of Nitrates: Role of Process Conditions and Co-Catalysts. ChemCatChem 2019;11:4642–52. https://doi.org/10.1002/cctc.201900890.

[16] Bahadori E, Tripodi A, Villa A, Pirola C, Prati L, Ramis G, et al. High pressure CO2 photoreduction using Au/TiO2: Unravelling the effect of co-catalysts and of titania polymorphs. Catal Sci Technol 2019;9:2253–65. https://doi.org/10.1039/c9cy00286c.

[17] Anas M, Han DS, Mahmoud K, Park H, Abdel-Wahab A. Photocatalytic degradation of organic dye using titanium dioxide modified with metal and non-metal deposition. Mater Sci Semicond Process 2015;41:209–18. https://doi.org/10.1016/j.mssp.2015.08.041.

[18] Bahadori E, Tripodi A, Villa A, Pirola C, Prati L, Ramis G, et al. High pressure photoreduction of CO2: Effect of catalyst formulation, hole scavenger addition and operating conditions. Catalysts 2018;8:430. https://doi.org/10.3390/catal8100430.

[19] Kumar SG, Devi LG. Review on modified TiO2 photocatalysis under UV/visible light: Selected results and related mechanisms on interfacial charge carrier transfer dynamics. J Phys Chem A 2011. https://doi.org/10.1021/jp204364a.

[20] Yan H, Wang X, Yao M, Yao X. Band structure design of semiconductors for enhanced photocatalytic activity: The case of TiO2. Prog Nat Sci Mater Int 2013;23:402–7. https://doi.org/10.1016/j.pnsc.2013.06.002.

[21] Moss B, Lim KK, Beltram A, Moniz S, Tang J, Fornasiero P, et al. Comparing photoelectrochemical water oxidation, recombination kinetics and charge trapping in the three polymorphs of TiO2. Sci Rep 2017;7. https://doi.org/10.1038/s41598-017-03065-5.

[22] Conte F, Pellegatta V, Tripodi A, Ramis G, Rossetti I. Photo-oxidation of ammonia to molecular nitrogen in water under uv, vis and sunlight irradiation. Catalysts 2021;11. https://doi.org/10.3390/catal11080975.

[23] Bahadori E, Conte F, Tripodi A, Ramis G, Rossetti I. Photocatalytic Selective Oxidation of Ammonia in a Semi-Batch Reactor: Unravelling the Effect of Reaction Conditions and Metal Co-Catalysts. Catalysts 2021;11:209. https://doi.org/10.3390/catal11020209.

[24] Silva CG, Pereira MFR, Órfão JJM, Faria JL, Soares OSGP. Catalytic and photocatalytic nitrate reduction over Pd-Cu loaded over hybrid materials of multi-walled carbon nanotubes and TiO2. Front Chem 2018;6. https://doi.org/10.3389/fchem.2018.00632.

[25] Serpone N, Lawless D, Disdier J, Herrmann J-M. Spectroscopic, Photoconductivity, and Photocatalytic Studies of Ti02 Colloids: Naked and with the Lattice Doped with Cr3+, Fe3+, and V5+ Cations. 1994.

[26] Challagulla S, Tarafder K, Ganesan R, Roy S. All that Glitters Is Not Gold: A Probe into Photocatalytic Nitrate

 doi:10.20944/preprints202201.0355.v1

Reduction Mechanism over Noble Metal Doped and Undoped TiO_2. J Phys Chem C 2017;121:27406–16.

[27] Zhang F, Jin R, Chen J, Shao C, Gao W, Li L, et al. High photocatalytic activity and selectivity for nitrogen in nitrate reduction on Ag/TiO2 catalyst with fine silver clusters. J Catal 2005;232:424–31. https://doi.org/10.1016/j.jcat.2005.04.014.

[28] Adamu H, Shand M, Taylor RSF, Manyar HG, Anderson JA. Use of carbon-based composites to enhance performance of TiO2 for the simultaneous removal of nitrates and organics from aqueous environments. Environ Sci Pollut Res 2018;25:32001–14. https://doi.org/10.1007/s11356-018-3120-x.

[29] Bahadori E, Compagnoni M, Tripodi A, Freyria F, Armandi M, Bonelli B, et al. Photoreduction of nitrates from waste and drinking water. Mater Today Proc 2018;5:17404–13. https://doi.org/10.1016/j.matpr.2018.06.042.

[30] P25 - EVONIK n.d.

[31] Chiarello GL, Rossetti I, Forni L. Flame-spray pyrolysis preparation of perovskites for methane catalytic combustion. J Catal 2005;236:251–61.

[32] Compagnoni M, Lasso J, Di Michele AI, Rossetti I. Flame-pyrolysis-prepared catalysts for the steam reforming of ethanol. Catal Sci Technol 2016;6:6247–56. https://doi.org/10.1039/C5CY01958C.